

Observation of a Van Hove singularity in $\text{Bi}_2\text{Sr}_2\text{CaCu}_2\text{O}_{8+x}$ with angle-resolved photoemission

Jian Ma, C. Quitmann, and R.J. Kelley

*Department of Physics and Applied Superconductivity Center, 1150 University Avenue, University of Wisconsin-Madison,
Madison, Wisconsin 53706*

P. Alm eras, H. Berger, and G. Margaritondo

Institut de Physique Appliqu ee, Ecole Polytechnique F d rale, CH-1015 Lausanne, Switzerland

M. Onellion

*Department of Physics and Applied Superconductivity Center, 1150 University Avenue, University of Wisconsin-Madison,
Madison, Wisconsin 53706*

(Received 17 May 1994; revised manuscript received 19 August 1994)

We have performed high-energy-resolution angle-resolved photoemission studies of the normal-state band structure of oxygen-overdoped $\text{Bi}_2\text{Sr}_2\text{CaCu}_2\text{O}_{8+x}$. We find that there is an extended saddle-point singularity in the density of states along the Γ - \bar{M} - Z direction. The data also indicate that there is an asymmetry in the Fermi surface for both the Γ - \bar{M} - Z and perpendicular directions.

I. INTRODUCTION

The possibility of a Van Hove singularity has been of considerable interest since it was proposed as a means of enhancing the superconducting transition temperature T_c .¹⁻⁴ The idea is that the tendency toward superconductivity in a two-dimensional system can be enhanced when the Fermi level lies at or close to the energy of a logarithmic Van Hove singularity (VHS) in the density of states.^{2,4} Several investigators have studied such a mechanism for raising the superconducting transition temperature T_c (Refs. 5-9) and there has been indirect experimental evidence indicating the possibility of a Van Hove singularity.^{10,11} More recently, direct spectroscopic observations of a Van Hove singularity, in the $\text{YBa}_2\text{Cu}_3\text{O}_{7-x}$ and $\text{YBa}_2\text{Cu}_4\text{O}_8$ (YBCO's) systems have been reported.^{12,13} Gofron *et al.* show that there is an extended saddle point singularity along the Γ - Y direction in reciprocal space, centered at the Y -point.¹² This report motivated us to study the $\text{Bi}_2\text{Sr}_2\text{CaCu}_2\text{O}_{8+x}$ (Bi-2212) system.

Recently, Dessau *et al.*¹⁴ provided a report for the Bi-2212 system on a flat band along the Γ - \bar{M} - Z direction. They presented data from Γ point to \bar{M} point, but not beyond \bar{M} , along the Γ - \bar{M} - Z direction.¹⁴ By assuming a tetragonal Fermi surface, Ref. 14 reported on their inferred topology of the Fermi surface. The authors of Ref. 14 argued from their data that there were bands just above and just below the Fermi surface along the Γ - \bar{M} - Z direction.

In this paper, we report on the Fermi surface topology of Bi-2212 near the $(\pi, 0)(\bar{M})$ point in the Brillouin zone. Our data indicate that there is indeed an extended Van Hove singularity, similar to that reported on YBCO's. An earlier report on Bi-2212 (Ref. 14) did not provide conclusive evidence as to the Fermi surface topology. Fi-

nally, our data do not indicate any Fermi surface crossing along the Γ - \bar{M} - Z direction for the oxygen stoichiometry used in our samples. Specifically, we do not observe any indication of a band crossing from below to above the Fermi energy as suggested by Ref. 14.

In addition, our data indicate that the Fermi surface does *not* exhibit tetragonal symmetry, in direct contradiction to the suggestion of Ref. 14. Specifically, our data establish that the flat region around the \bar{M} point is not symmetric about \bar{M} . Further, the data indicate that the Γ - X and Γ - Y directions are inequivalent, consistent with all other earlier reports¹⁵⁻¹⁹ with one exception.¹⁴ Our data for directions parallel to Y - \bar{M} - X provide information essential to determining the topology of the Fermi surface, and also additional insight on the inequivalence of Γ - X and Γ - Y .

II. EXPERIMENTAL

The experiments were performed using the 4-m normal incidence monochromator at the Wisconsin Synchrotron Radiation Center in Stoughton, WI. The beam line provides highly (> 95%) linearly polarized light with the electric vector in the horizontal plane and with photon energy resolution better than 10 meV. The angle-resolved photoemission chamber includes a reverse-view low-energy electron diffraction (LEED) optics used to orient the sample *in situ* after cleaving. The electron energy analyzer is a 50 mm VSW hemispherical analyzer mounted on a two-axis goniometer, with an acceptance full angle of 2° . The base pressure is 6×10^{-11} torr. The incidence angle between the photon Poynting vector and surface normal was 45° unless otherwise noted.

The single-crystal samples were annealed in 1 atm of oxygen at 530°C for 20 h. Figure 1 illustrates the re-

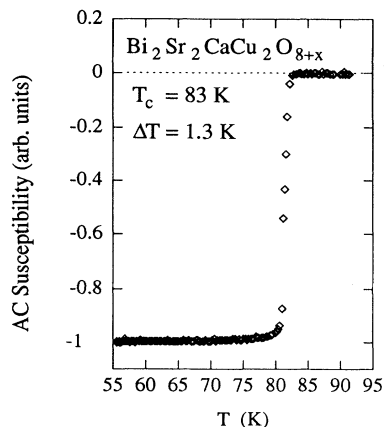


FIG. 1. ac susceptibility data for an oxygen-overdoped $\text{Bi}_2\text{Sr}_2\text{CaCu}_2\text{O}_{8+x}$ single crystal annealed in 1 atm O_2 at 530°C for 20 h. The onset T_c is 83 K, with 10–90% transition width $\Delta T = 1.3$ K.

sults of ac susceptibility measurements. Note particularly that T_c is 83 K and the 10–90% temperature width is 1.3 K. The crystals were characterized using four-point resistivity, x-ray diffraction, and transmission electron microscopy. The samples were transferred from a load lock chamber with a base pressure of 5×10^{-9} torr to the main chamber, and cleaved at 30 K in a vacuum of $6\text{--}8 \times 10^{-11}$ torr. The sample holder includes the capability to rotate the sample *in situ* about the surface normal, at low temperatures, for precision alignment with respect to the photon electric field. To measure the normal-state electronic band structure, the temperature was raised to 95 K, above T_c . The stability of the temperature was ± 1 K. We obtained a Fermi edge reference by using the spectra of freshly deposited gold films. An energy resolution of 15 meV was achieved using 1 eV pass energy. For the present study, the overall energy resolution employed was 35 meV unless otherwise stated.

For a quasi-two-dimensional system such as $\text{Bi}_2\text{Sr}_2\text{CaCu}_2\text{O}_{8+x}$ the initial state of the electron can be determined by measuring the component of the electron momentum parallel to the sample surface (\mathbf{k}_{\parallel}). By measuring the energy distribution curves (EDC's) for different directions (θ , ϕ) of the emitted photoelectron relative to the surface normal, the \mathbf{k}_{\parallel} of the initial state is derived from the relation $\mathbf{k}_{\parallel} = (0.512 \text{ \AA}^{-1})\sqrt{E_{\text{kin}}}(\sin\theta \cos\phi \hat{k}_x + \sin\phi \hat{k}_y)$, where E_{kin} is the kinetic energy of measured photoelectrons in the unit of eV, and \hat{k}_x and \hat{k}_y denote unit vectors along two Cu-O bond axis (Γ - \bar{M} directions). We used the measured work function of 4.35 ± 0.050 eV. Our uncertainty in \mathbf{k}_{\parallel} is $\pm 0.037 \text{ \AA}^{-1}$.

We employed *in situ* low-energy electron diffraction (LEED) to align the samples. We further confirmed the alignment by determining the symmetric point of the Fermi surface crossings along the X - Γ - X line, where the dispersion is rapid. Our sample alignment uncertainty is $\pm 1^\circ$, using the Fermi surface crossings.

To estimate the binding energies, we determined the angles at which the dispersing state is clearly cut off by

the Fermi energy for the first time. These spectra are assigned a binding energy of 0 meV. All other binding energies are assigned by comparing to these spectra. Since the peak is broad, we could only obtain an uncertainty in binding energy of ± 20 meV, although our step size in the spectra is 5 meV.

We also obtained the Fermi energy using a second, independent, method. We deposited a fresh gold film onto a gold sheet that was in electrical contact with the sample, and located 2 cm below, and coaxial with, the sample. We measured the Fermi energy of the gold film by obtaining a photoemission spectrum of the film. The two methods of estimating the Fermi energy agreed to within 10 meV.

III. RESULTS AND DISCUSSION

We first oriented the sample so that the Γ - \bar{M} - Z direction was in the horizontal plane. We measured the dispersion of the normal-state quasiparticle band along the Γ - \bar{M} - Z horizontal axis. Figures 2(a) and 2(b) illustrate the spectra obtained using an energy resolution of (a) 55 meV and (b) 35 meV, and a photon energy of (a) 21 eV and (b) 25 eV. The emission angle of the photoelectrons for each spectrum is noted in the figure.

A band develops and is visible for 8° off normal at a binding energy of 335 ± 35 meV. The band disperses toward the Fermi energy and, at $\theta = 20^\circ$, is at a binding energy of 0–20 meV. The estimates of the binding energy are limited by the width of the spectral features. The \bar{M} point at the photon energy of 25 eV is at 21° . For this polarization (even symmetry) there is no indication of a Fermi level crossing,²⁰ consistent with reports of Dessau *et al.*¹⁴

Between $\theta = 20^\circ$ and 32° the quasiparticle band remains at a binding energy of 0–20 meV. Starting at 34° the quasiparticle band disperses to higher binding energy, reaching a binding energy of 120 meV at an angle of 40° . The dispersion curve is illustrated in Fig. 2(c). The data in Fig. 2 illustrate an observation for BSCCO-(2212) of the quasiparticle dispersion away from the Fermi energy along the \bar{M} - Z line. In particular, note that our data extend well beyond the \bar{M} point, and provide clear indication of dispersion away from the Fermi energy going from \bar{M} to both Γ and Z . Earlier reports¹⁴ provided data only from Γ - \bar{M} . All of the above results on the quasiparticle dispersion along the Γ - \bar{M} - Z direction were confirmed using a photon energy of 21 eV. This behavior, with the quasiparticle band near the Fermi energy for an extended portion of the Γ - \bar{M} - Z line, is consistent with an extended saddle-point singularity.¹² Note also that the dispersion is not symmetric with respect to the \bar{M} point; we return later to this point. Because this asymmetry with respect to the \bar{M} point is important, we carefully confirmed, by checking Fermi surface crossings along the Γ - X direction, that the degree of sample misalignment ($\pm 1^\circ$, as noted above) could not account for the observed asymmetry about the \bar{M} point.

The other crucial issue of the band structure topology is the behavior of the quasiparticle band along cuts per-

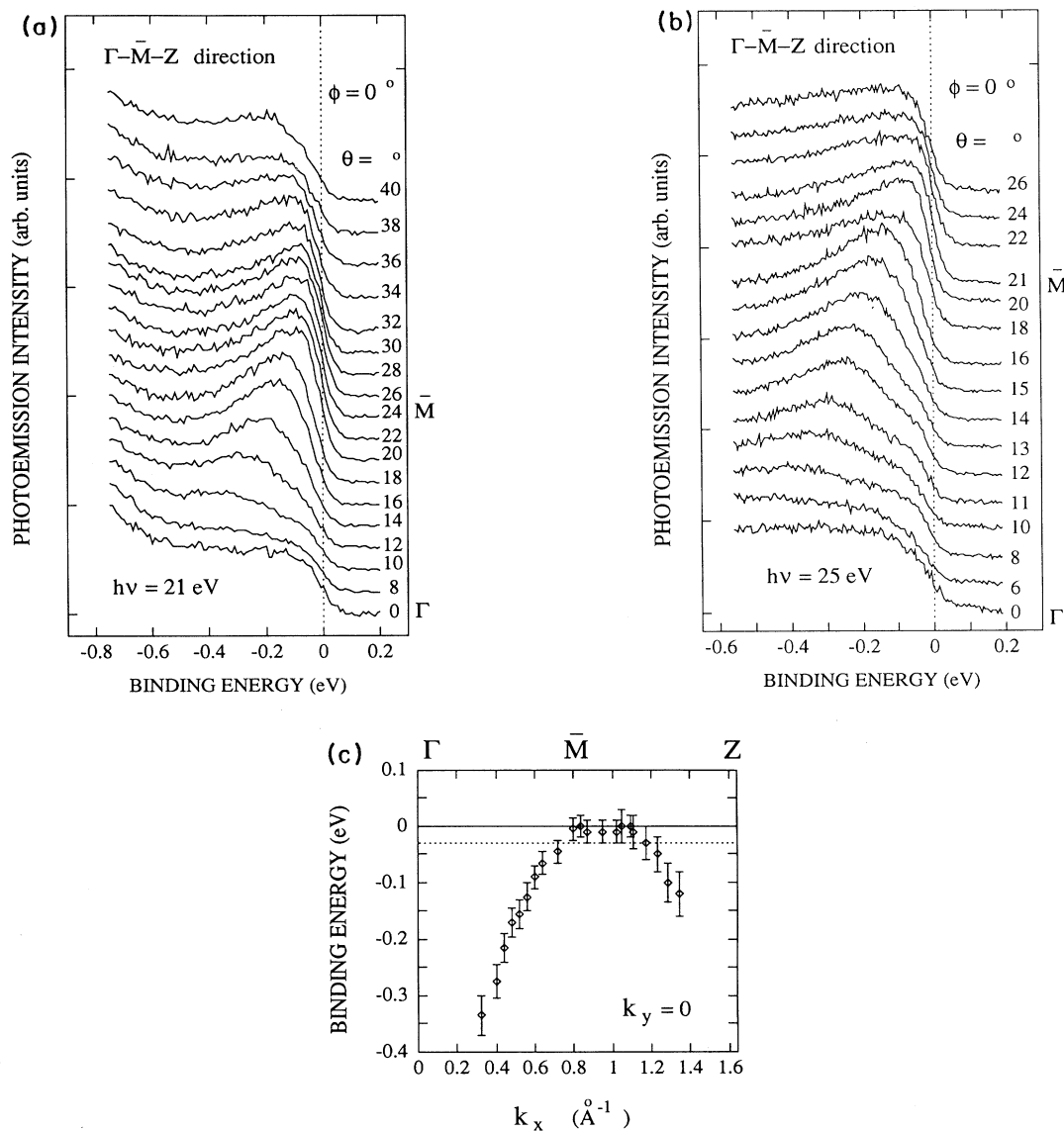


FIG. 2. Normal-state ($T=95$ K) angle-resolved photoemission spectra for an oxygen-overdoped $\text{Bi}_2\text{Sr}_2\text{CaCu}_2\text{O}_{8+x}$ single crystal of $T_c = 83$ K along the Γ - \bar{M} -Z direction in the Brillouin zone. The Γ - \bar{M} -Z direction lies in the photon polarization plane (even symmetry). Photon energy of (a) 21 eV, (b) 25 eV employed. (c) Dispersion curve obtained from (a) and (b). The results for $0 \leq k_x \leq 1.09 \text{ \AA}^{-1}$ are taken, one for one, from the spectra of (b), while the results for $1.09 \text{ \AA}^{-1} \leq k_x$ are taken from the spectra of (a). Note the dispersing electronic state that disperses toward the Fermi energy E_f away from Γ , the extended flat region between 0.75 - 1.25 \AA^{-1} , and the dispersion away from E_f at wave vectors greater than 1.25 \AA^{-1} . The dotted line indicates the maximum binding energy for which a photoemission superconducting condensate peak is observed (Ref. 22).

pendicular to the Γ - \bar{M} -Z direction. To obtain definitive information, we made four cuts, at angles 14° , 16° , 18° , and 20° along the Γ - \bar{M} -Z direction. In Figs. 3–6, we illustrate the results obtained with 25 eV photon energy. We also confirmed the results of Figs. 3–6 by using a photon energy of 21 eV (data not shown). Figures 3(a) and 3(b) illustrate the results for the cut at $\theta = 20^\circ$, very close to the \bar{M} point along the Γ - \bar{M} -Z line. Figure. 3(a) illustrates the spectra along the Y - \bar{M} - X line. Along the \bar{M} - X line, the intensity of the quasiparticle

band decreases monotonically with increasing angle. At $\phi = -5^\circ$ only the background remains. The data indicate that the band disperses up through the Fermi energy almost immediately as one moves from \bar{M} along the \bar{M} - X line. By contrast, along the \bar{M} - Y line, the band first disperses slightly away from the Fermi surface and then exhibits a clear Fermi surface crossing between $\phi = +7^\circ$ and $+9^\circ$. Figure 3(b) illustrates the dispersion along the X - \bar{M} - Y direction, with Fermi surface crossings as one moves away from the \bar{M} point in either direction, but

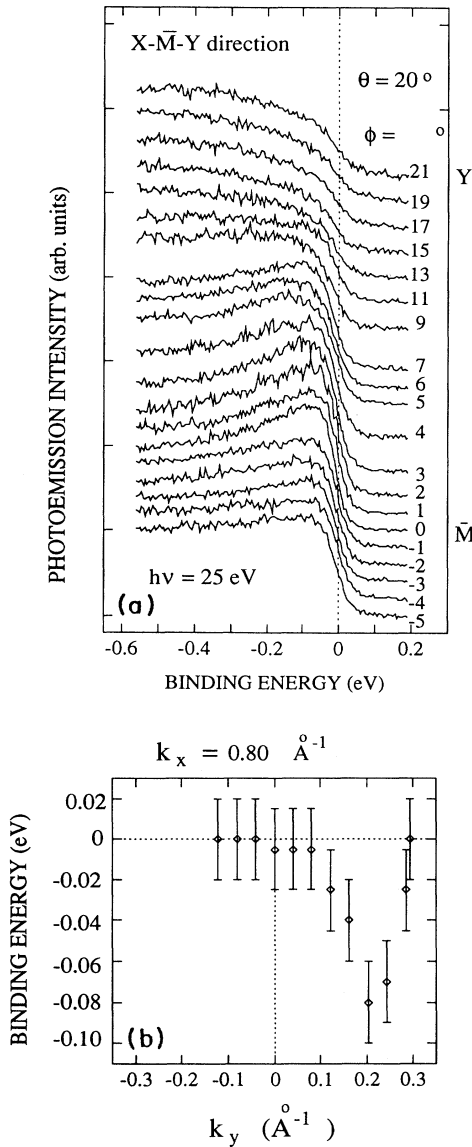


FIG. 3. (a) Normal-state ($T=95$ K) angle-resolved photoemission spectra for an oxygen-overdoped $\text{Bi}_2\text{Sr}_2\text{CaCu}_2\text{O}_{8+x}$ single crystal of $T_c = 83$ K along the $\Gamma\text{-}\bar{M}\text{-}Z$ direction. k_x is 0.80 \AA^{-1} . The $\Gamma\text{-}\bar{M}\text{-}Z$ direction lies in the photon polarization plane (even symmetry). A photon energy of 25 eV was employed. (b) The dispersion curve obtained from (a). Positive values of k_y correspond to a wave vector pointed along the $\bar{M}\text{-}Y$ direction. Negative values of k_y correspond to negative angles in (a).

the Fermi surface crossings in the $\bar{M}\text{-}X$ and $\bar{M}\text{-}Y$ directions are not symmetric with respect to the $\Gamma\text{-}\bar{M}\text{-}Z$ line.

Another noteworthy point about Fig. 3(a) is that we obtained data all the way from the \bar{M} point to the Y point. Notice that there is only one Fermi surface crossing visible along $\bar{M}\text{-}Y$ in the data. If there was a Bi pocket, one would expect two Fermi surface crossings along $\bar{M}\text{-}Y$. Our data indicate that there is no Bi pocket around the \bar{M} point for this stoichiometry.²¹

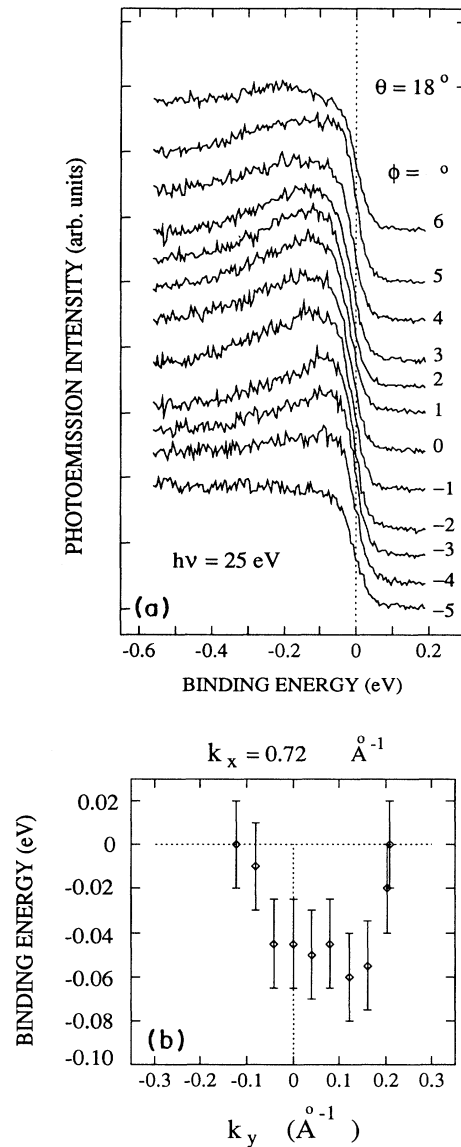


FIG. 4. (a) Normal-state (95 K) angle-resolved photoemission spectra for an oxygen-overdoped $\text{Bi}_2\text{Sr}_2\text{CaCu}_2\text{O}_{8+x}$ single crystal of T_c along a direction parallel to the $X\text{-}\bar{M}\text{-}Y$ direction at $\theta = 18^\circ$. k_x is 0.72 \AA^{-1} . The $\Gamma\text{-}\bar{M}\text{-}Z$ direction lies in the photon polarization plane (even symmetry). The photon energy was 25 eV. (b) The dispersion curve obtained from (a). Positive values of k_y correspond to a wave vector parallel to the $\bar{M}\text{-}Y$ direction. Negative values of k_y correspond to negative angles in (a).

Figure 4 illustrates the cut at 18° parallel to the $X\text{-}\bar{M}\text{-}Y$ line. The spectra in Fig. 4(a) exhibit an abrupt reduction in the quasiparticle spectral feature intensity between $\theta/\phi = 18^\circ/ -4^\circ$ and $\theta/\phi = 18^\circ/ -5^\circ$ in going toward X , but the corresponding Fermi surface crossing in going toward Y occurs between $\theta/\phi = 18^\circ/5^\circ$ and $\theta/\phi = 18^\circ/6^\circ$. Figure 4(b) illustrates the details of the dispersion observed in Fig. 4(a). Note in particular that the dispersion is again asymmetric about the $\Gamma\text{-}\bar{M}\text{-}Z$

line, with a maximum binding energy of 60 meV at $\phi = +3^\circ$. Also, it is noteworthy that for this cut, again, the quasiparticle state disperses above the Fermi energy as one moves away from the Γ - \bar{M} - Z line in either direction.

We also studied a cut at $\theta = 16^\circ$ parallel to the X - \bar{M} - Y line. Figure 5(a) illustrates the spectra, and Fig. 5(b) the resulting dispersion relation. For this cut, the dispersion is almost symmetric, with a saddle point centered at $\phi = -1^\circ$. Note that the quasiparticle state again disperses above the Fermi energy as one moves away from the Γ -

\bar{M} - Z line in either direction. The results of the cuts at 16° , 18° , and 20° all indicate that the Fermi surface topology is markedly different around the X and the Y points.

Figure 6 illustrates a cut at $\theta = 14^\circ$ parallel to the X - \bar{M} - Y line. Note that the binding energy, 130 meV, along the Γ - \bar{M} - Z line for this cut places the quasiparticle state well below the Fermi energy. For this reason, we would expect the behavior of the quasiparticle state in this part of the Brillouin zone not to be strongly involved

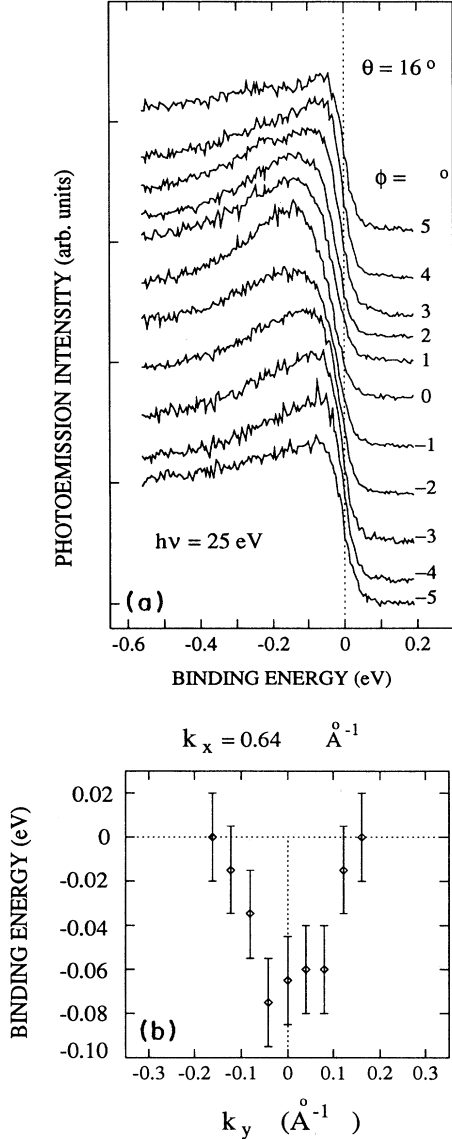


FIG. 5. (a) Normal-state (95 K) angle-resolved photoemission spectra for an oxygen-overdoped $\text{Bi}_2\text{Sr}_2\text{CaCu}_2\text{O}_{8+x}$ single crystal $T_c = 83$ K along a direction parallel to the X - \bar{M} - Y line at $\theta = 16^\circ$. k_x is 0.64 \AA^{-1} . The Γ - \bar{M} - Z direction lies in the photon polarization plane (even symmetry). The photon energy was 25 eV. (b) The dispersion curve obtained from (a). Positive values of k_y correspond to a wave vector parallel to the \bar{M} - Y direction. Negative values of k_y correspond to negative angles in (a).

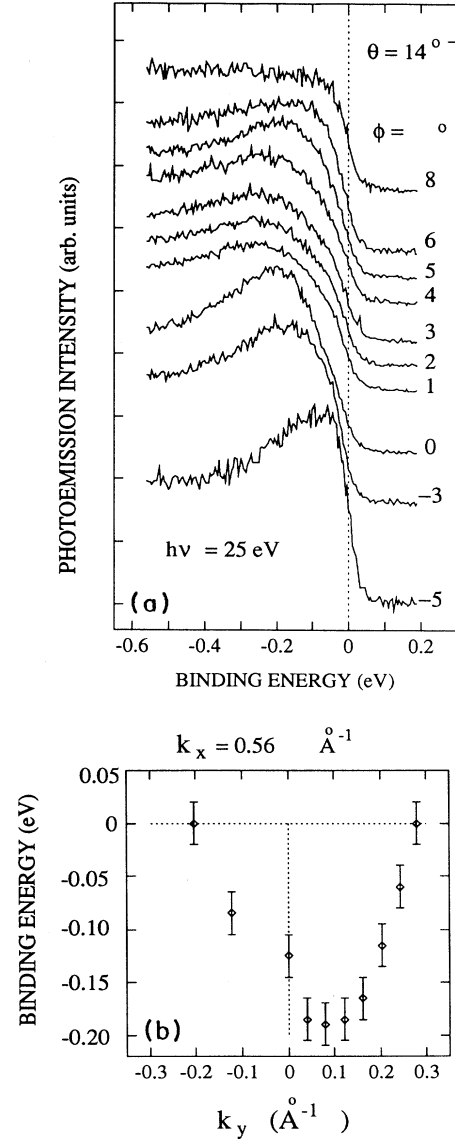


FIG. 6. (a) Normal-state (95 K) angle-resolved photoemission spectra for an oxygen-overdoped $\text{Bi}_2\text{Sr}_2\text{CaCu}_2\text{O}_{8+x}$ single crystal of $T_c = 83$ K along a direction parallel to the X - \bar{M} - Y direction at $\theta = 14^\circ$. k_x is 0.56 \AA^{-1} . The Γ - \bar{M} - Z direction lies in the photon polarization plane (even symmetry). The photon energy was 25 eV. (b) The dispersion curve obtained from (a). Positive values of k_y correspond to a wave vector parallel to the \bar{M} - Y direction. Negative values of k_y correspond to negative angles in (a).

in the superconducting properties. Note, however, that we observe asymmetric Fermi surface crossings along this cut at $\theta/\phi = 14^\circ / -5^\circ$ and at $\theta/\phi = 14^\circ / +7^\circ$, another indication that the shape of the Fermi surface around the X and the Y points is different.

Figure 7 summarizes (a) our partial Fermi surface mapping and (b) the shape of the Fermi surface near the Γ - \bar{M} - Z direction. The mapping is a purely experimental derivation; we have made no *a priori* assumptions regarding the symmetry of the Fermi surface. As noted above, we observe an asymmetric Fermi surface shape with respect to the \bar{M} point along the Γ - \bar{M} - Z line. The cause of this asymmetry is unknown; however, our observations are consistent with our finding that the Γ - Y and Γ - X lines are inequivalent.¹⁵ Note also that the shape of the Fermi surface is as expected for an extended saddle-point type of Van Hove singularity. The asymmetry between \bar{M} - Y and \bar{M} - X is important for deciding what basis to employ for models of the Fermi surface. For that rea-

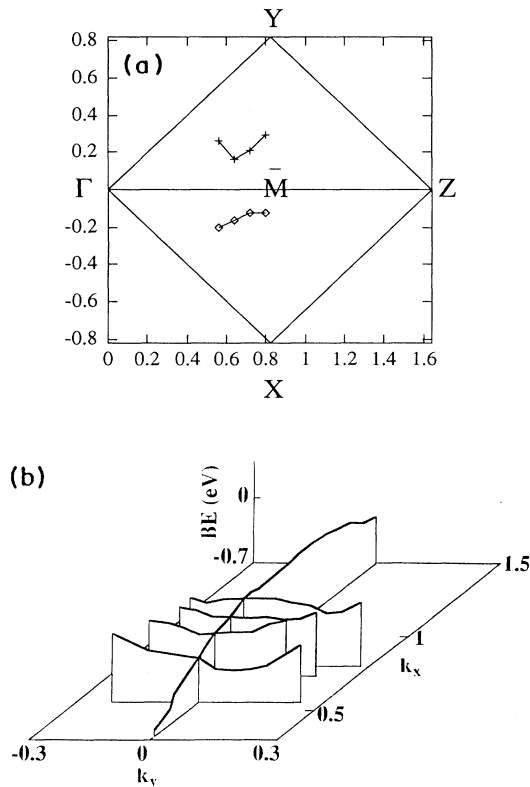


FIG. 7. (a) The experimental positions of the Fermi surface crossings near the Γ - \bar{M} - Z direction. The sample exhibits orthorhombic, not tetragonal, symmetry, in agreement with structural characterization. The plane containing the c axis and the Γ - \bar{M} - Z direction is not a plane of reflection symmetry of the Fermi surface. (b) The perspective drawing of the binding energy of the spectral features near the Γ - \bar{M} - Z direction. Note that the band disperses through the Fermi energy as one moves away from the Γ - \bar{M} - Z line in either perpendicular direction, as expected for an extended saddle-point Van Hove singularity.

son, as mentioned above, we carefully checked our sample alignment. The difference between \bar{M} - Y and \bar{M} - X crossings varies from 4° [Fig. 7(a), 20° cut, and Fig. 3] to 0° [Fig. 7(a), 16° cut, and Fig. 5]. It is not possible to account for this asymmetry in Fermi surface crossings by sample misalignment, which would rigidly shift all such crossings. Instead, the data indicate that the \bar{M} - Y and

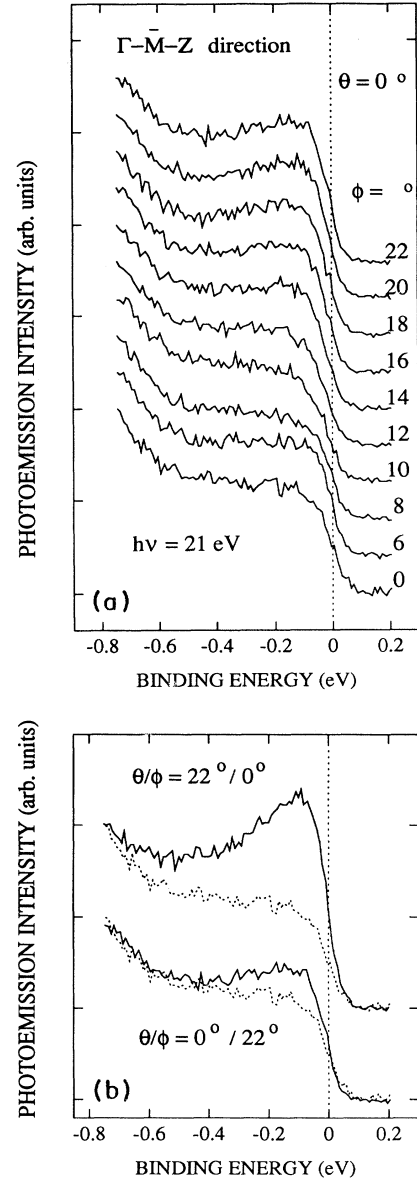


FIG. 8. (a) Normal state ($T = 95$ K) angle-resolved photoemission spectra for an oxygen-overdoped $\text{Bi}_2\text{Sr}_2\text{CaCu}_2\text{O}_{8+\delta}$ single crystal of $T_c = 83$ K along the Γ - \bar{M} - Z direction in the Brillouin zone. The Γ - \bar{M} - Z direction lies perpendicular to the photon polarization plane (odd symmetry). The photon energy was 21 eV. Note the loss of spectral intensity compared to Fig. 2(a). (b) Direct comparison of the spectra taken for two orientations (odd and even). The dotted lines are the spectra taken at normal emission. All spectra have been normalized above the Fermi energy and at high binding energy.

\bar{M} - X directions are inequivalent, consistent with earlier reports.^{15–19}

Our results are different from those reported by Ref. 14 who, however, studied more lightly doped samples (ours are overdoped with oxygen), and who incorrectly assumed tetragonal symmetry. The authors of Ref. 14 symmetrized their data, assuming tetragonal symmetry, rather than obtaining actual experimental measurements for all parts of the Brillouin zone shown in Ref. 15. Our data establish that for the overdoped samples, the Fermi surface exhibits orthorhombic, rather than tetragonal, symmetry. Such a result is consistent with x-ray and transmission electron microscopy studies of our crystals, which both indicate orthorhombic symmetry. Earlier reports indicate that the orthorhombic structure arises from a Bi-O buckling distortion that also affects the CuO_2 planes.²³

In addition to revealing the extended saddle-point Van Hove singularity, our data allow us to comment on the possibility of an electronic state just above the Fermi energy in the Γ - \bar{M} - Z direction. Recently, Ref. 14 argued that on optimally doped $\text{Bi}_2\text{Sr}_2\text{CaCu}_2\text{O}_x$ samples there are two closely spaced electronic states, one of even and the other of mixed symmetry. Along the Γ - \bar{M} - Z direction and with even symmetry orientation, our data are, for the wave-vector domain in common, similar to those reported by Ref. 14. However, as illustrated in Fig. 8, along the Γ - \bar{M} - Z direction and with odd symmetry orientation, we find a less intense (by a factor of 5) electronic state. We emphasize that we do not observe a clear Fermi surface crossing, for either polarization, along the Γ - \bar{M} - Z direction. Our data are inconsistent with the band structure, and tetragonal symmetry, proposed in Ref. 14.

To ensure that this is not due to a matrix element effect, we took data at several photon energies in the 17–30 eV range. The difference noted in Fig. 8 is independent of the photon energy.

If we define a polarization factor $P = (S_{\theta=22^\circ} - S_{\phi=22^\circ}) / (S_{\theta=22^\circ} + S_{\phi=22^\circ})$, where S_θ and S_ϕ represent the photoemission spectral area at θ and ϕ after the subtraction of normal emission spectral area, respectively, the data indicate that for the overdoped samples, the electronic state along the Γ - \bar{M} - Z direction is $P = 66\%$ of even symmetry, as indicated in Fig. 8(b). This result contrasts to that of Ref. 14 who, for different stoichiometry samples, report an electronic state in the odd symmetry orientation that disperses through the Fermi surface along the Γ - \bar{M} - Z direction.

The two data sets indicate that the oxygen doping affects the symmetry of the quasiparticle state along the Γ - \bar{M} - Z direction. Our results, illustrated in Fig. 8 and repeatedly reproduced for overdoped samples, establish that the quasiparticle state exhibits almost perfect even symmetry in the Γ - \bar{M} - Z direction. We emphasize that our data for overdoped samples do not allow us to confirm or to exclude the possibility of a mixed-symmetry state, observable in odd symmetry orientation, that disperses through the Fermi surface. We simply do not observe any strong state in the odd symmetry orientation.

IV. CONCLUSION

We have mapped the quasiparticle dispersion along the Γ - \bar{M} - Z direction up to nearly the Z point. We find an extended saddle-point type of singularity in the Fermi surface, which can lead to a stronger than logarithmic enhancement of T_c . It is noteworthy, as Abrikosov has pointed out, that this enhancement is virtually independent of the choice of exchange boson. Our experimental data are also in agreement with the recent work of Dagotto *et al.*,²⁴ who argue that the dispersion and flat region along the Γ - \bar{M} - Z direction are an effect of electron-electron correlation. We have found that the overdoped $\text{Bi}_2\text{Sr}_2\text{CaCu}_2\text{O}_{8+x}$ system exhibits an orthorhombic, rather than a tetragonal, Fermi surface.

After submitting this report, we received a copy of an unpublished manuscript by J. Osterwalder *et al.*,¹⁷ previously unknown to us. We also note the recent publication by Yokoya *et al.*¹⁸ Both research groups also report that the electronic band structure exhibits orthorhombic, rather than tetragonal, symmetry.

ACKNOWLEDGMENTS

We benefited from conversations with Andrey Chubukov, Robert Joynt, Alexei Abrikosov, Elbio Dagotto, and Philippe Aebi. The staff at the Wisconsin Synchrotron Radiation Center, particularly Tom Baraniak, were most helpful. Financial support was provided by the U.S. NSF, both directly (DMR-9214707) and through support of the SRC, by Ecole Polytechnique Fédérale Lausanne and the Fonds National Suisse de la Recherche Scientifique, and by the Deutsche Forschungsgemeinschaft.

¹ For a review of Van Hove scenarios in cuprate superconductors, see D.M. Newns, C.C. Tsuei, P.C. Pattnaik, and C.L. Kane, *Comments Condens. Matter Phys.* **15**, 273 (1992).

² J.E. Hirsh and D.J. Scalapino, *Phys. Rev. Lett.* **56**, 2732 (1986).

³ J. Labbe and J. Bok, *Europhysics Lett.* **3**, 1225 (1987).

⁴ J. Friedel, *J. Phys. Condens. Matter* **1**, 7757 (1989).

⁵ R.S. Markiewicz and B.G. Giessen, *Physica C* **160**, 497 (1989).

⁶ A.A. Abrikosov, J.C. Campuzano, and K. Gofron, *Physica C* **214**, 73 (1993).

⁷ D.M. Newns, H.R. Krishnamurthy, P.C. Pattnaik, C.C. Tsuei, and C.L. Kane, *Phys. Rev. Lett.* **69**, 1264 (1992).

⁸ S. Takács, *Phys. Rev. B* **48**, 13127 (1993).

- ⁹ R.J. Radtke and M.R. Norman (unpublished).
- ¹⁰ C.C. Tsuei, C.C. Chi, D.M. Newns, P.C. Pattnaik, and M. Däumling, *Phys. Rev. Lett.* **69**, 2134 (1992).
- ¹¹ P.C. Pattnaik, C.L. Kane, D.M. Newns, and C.C. Tsuei, *Phys. Rev. B* **45**, 5714 (1992).
- ¹² K. Gofron, J.C. Campuzano, R. Liu, H. Ding, D. Koelling, A.A. Abrikosov, B. Dabrowski, and B.W. Veal (unpublished).
- ¹³ Rong Liu, B.W. Veal, A.P. Paulikas, J.W. Downey, P.J. Kostić, S. Fleshler, U. Welp, C.G. Olson, X. Wu, A.J. Arko, and J.J. Joyce, *Phys. Rev. B* **46**, 11056 (1992).
- ¹⁴ D.S. Dessau, Z.-X. Shen, D.M. King, D.S. Marshall, L.W. Lombardo, P.H. Dickinson, A.G. Loeser, J. DiCarlo, C.-H. Park, A. Kapitulnik, and W.E. Spicer, *Phys. Rev. Lett.* **71**, 2781 (1993).
- ¹⁵ R.J. Kelley, Jian Ma, M. Onellion, M. Marsi, P. Alméras, H. Berger, and G. Margaritondo, *Phys. Rev. B* **48**, 3534 (1993).
- ¹⁶ P. Aebi, J. Osterwalder, P. Schwaller, L. Schlapbach, M. Shimoda, T. Mochiku, and K. Kadowaki, *Phys. Rev. Lett.* **72**, 2757 (1994).
- ¹⁷ J. Osterwalder, P. Aebi, P. Schwaller, L. Schlapbach, M. Shimoda, T. Mochiku, and K. Kadowaki, *Appl. Phys. A* (to be published).
- ¹⁸ T. Yokoya, T. Takahashi, T. Mochiku, and K. Kadowaki, *Phys. Rev. B* **50**, 10225 (1994).
- ¹⁹ J.C. Campuzano (private communication).
- ²⁰ C.G. Olson, R. Liu, D.W. Lynch, R.S. List, A.J. Arko, B.W. Veal, Y.C. Chang, P.Z. Jiang, and A.P. Paulikas, *Phys. Rev. B* **42**, 381 (1990).
- ²¹ S. Massidda, Jaejun Yu, and A.J. Freeman, *Physica C* **152**, 251 (1988).
- ²² Jian Ma, C. Quitmann, R.J. Kelley, H. Berger, G. Margaritondo, and M. Onellion, *Science* (to be published).
- ²³ M.D. Kirk, J. Nogami, A.A. Baski, D.B. Mittzi, A. Kapitulnik, T.H. Geballe, and C.F. Quate, *Science* **242**, 1673 (1988), and references therein.
- ²⁴ E. Dagotto, A. Nazarenko, and M. Boninsegni, *Phys. Rev. Lett.* **73**, 728 (1994).